Cell Surface Changes and Enzyme Release during Hypoxia and Reoxygenation in the Isolated, Perfused Rat Liver

JOHN J. LEMASTERS, CAROLE J. STEMKOWSKI, SUNGCHUL JI, and RONALD G. THURMAN

Laboratories for Cell Biology, Department of Anatomy, and Department of Pharmacology, School of Medicine, University of North Carolina at Chapel Hill, Chapel Hill, North Carolina 27514.
Dr. Ji's present address is Department of Pharmacology, College of Pharmacy, Rutgers University, Piscataway, New Jersey 08859.

ABSTRACT We examined the effects of hypoxia and reoxygenation in isolated, perfused rat livers. Hypoxia induced by a low rate of perfusion led to near anoxia confined to centrilobular regions of the liver lobule. Periportal regions remained normoxic. Within 15 min, anoxic centrilobular hepatocytes developed surface blebs that projected into sinusoids through endothelial fenestrations. Periportal hepatocytes were unaffected. Both scanning and transmission electron microscopy suggested that blebs developed by transformation of preexisting microvilli. Upon reoxygenation by restoration of a high rate of perfusion, blebs disappeared. Other changes included marked shrinkage of hepatocytes, enlargement of sinusoids, and dilation of sinusoidal fenestrations. There was also an abrupt increase in the release of lactate dehydrogenase and protein after reoxygenation, and cytoplasmic fragments corresponding in size and shape to blebs were recovered by filtration of the effluent perfusate.

We also studied phalloidin and cytochalasin D, agents that disrupt the cytoskeleton. Both substances at micromolar concentrations caused rapid and profound alterations of cell surface topography.

We conclude that hepatic tissue is quite vulnerable to hypoxic injury. The morphological expression of hypoxic injury seems mediated by changes in the cortical cytoskeleton. Reoxygenation causes disappearance of blebs and paradoxically causes disruption of cellular volume control and release of blebs as cytoplasmic fragments. Such cytoplasmic shedding provides a mechanism for selective release of hepatic enzymes by injured liver tissue.

Liver microcirculation is best understood in terms of the lobule, the basic anatomical unit of the liver. Blood enters the periphery of the lobule via the hepatic artery and portal vein. It continues through sinusoids, the specialized capillaries of the liver, and drains into the central vein at the lobule's center. Since various substances are removed or added to blood during its passage through the liver lobule, gradients of metabolic substrates, waste products, hormones, internal secretions, and so forth are created. Oxygen, in particular, is extracted during its passage through the liver. In vivo, an oxygen gradient of 40 to 60 torr exists across the lobule indicative of a high degree of oxygen extraction from the blood (1). In addition to these flow-induced gradients, there are numerous important structural, biochemical, and functional differences between the various regions of the liver lobule (2–4). Based on the lobular distribution of hepatic enzymes, Jungermann and Sasse (4) concluded that periportal hepatocytes are adapted to gluconeogenic and oxidative processes, whereas centrilobular hepatocytes are specialized for glycolysis.

Since oxygen consumption and extraction by the liver is high, it is not surprising that oxygen deficits have been implicated in certain types of liver injury, especially in centrilobular regions which are furthest from the oxygen supply (5, 6). However, since centrilobular hepatocytes seem especially well adapted for glycolysis, they may not be particularly vulnerable to hypoxic injury. Recently, we developed techniques for monitoring metabolism and oxygen concentration within different regions of the liver lobule using miniature probes (7–10). In a preliminary report (10), we demonstrated that inadequate oxygen delivery to the isolated, perfused rat liver led to selective centrilobular anoxia and injury in which the normoxic periportal hepatocytes were spared. In the present report we provide a detailed account of the onset, evolution,

THE JOURNAL OF CELL BIOLOGY · VOLUME 97 SEPTEMBER 1983 778–786

and reversibility of hypoxic hepatic injury. The data indicate that anoxic stress leads to prominent alterations of the hepatocellular cell surface mediated, apparently, by a disruption of the underlying cortical cytoskeleton. Reoxygenation, while reversing some of the cell surface changes, causes disruption of cellular volume control and leads to the shedding of cytoplasmic fragments into the microcirculation. This latter effect could be responsible for the appearance of hepatic enzymes in the blood after liver injury.

MATERIALS AND METHODS

Liver Perfusion: Livers from fed, male Sprague-Dawley rats (200–275 g) were perfused at 37°C with hemoglobin-free Krebs-Henseleit-bicarbonate buffer (118 mM NaCl, 24.9 mM $NaHCO_3$, 1.19 mM KH_2PO_4, 1.18 mM $MgSO_4$, 4.74 mM KCl, and 1.27 mM $CaCl_2$ saturated with 95% oxygen, 5% carbon dioxide, pH 7.4) essentially as described by Scholz et al. (11). Briefly, the abdomen was opened under sodium pentobarbital anesthesia (65 mg/kg body weight), and perfusate was pumped into the liver via a cannula placed in the portal vein. Effluent was collected from a second cannula placed in the vena cava through the right atrium. After tying off the inferior vena cava, the liver was severed from its retroperitoneal attachments and removed from the carcass. For most experiments, the liver was mounted in a shallow basin containing perfusion medium. Such flotation seemed to provide the most even distribution of perfusate to the various lobes. During surgery, perfusion rates were kept moderately low (~2 ml/min/g of liver) until the effluent cannula was inserted and secured. Thereafter, the perfusion rate was 3–4 ml/min/g unless otherwise specified. Perfusate was not recirculated.

Effluent was passed by a Teflon-shielded Clark-type oxygen electrode (12). Respiratory rates averaged ~2 μmol/min/g of liver as calculated from the portal-caval oxygen concentration difference, the flow rate, and the liver weight. Liver weight was assumed to be 4% of body weight.

Surface fluorescence of pyridine nucleotides was measured with multi-fiber lightguides or with two-fiber micro-lightguides placed on the surface of the liver as previously described (7). Pyridine nucleotide fluorescence was used as an indirect signal for tissue oxygenation with an increase in fluorescence signifying cellular anoxia (13).

Electron Microscopy: Livers were fixed by switching to a perfusion medium containing, in addition, 2% glutaraldehyde and 2% paraformaldehyde. For scanning electron microscopy, tissue was cut into 1-cm cubes and placed overnight in cold secondary fixative containing 2% glutaraldehyde, 0.1 M NaPi buffer, pH 7.4. Subsequently, the tissue was washed in water, dehydrated in 2,2-dimethoxypropane, and critical-point dried in carbon dioxide. The dried tissue was cut manually with a razor blade, mounted on an aluminum stub, and coated with gold-palladium using a sputter evaporator for viewing with a JEOL 35C scanning electron microscope. For transmission electron microscopy, tissue was cut into 1-mm cubes and fixed an additional 2 h in cold 2% glutaraldehyde, 2% tannic acid, 0.1 M NaPi buffer, pH 6.5. Subsequent steps of postosmication, embedding in epon, thin sectioning, and staining with lead and uranyl salts were performed by standard techniques. Thin sections so prepared were viewed with a JEOL 100CX electron microscope.

Some effluents were passed through polycarbonate filters of 0.2 μm pore diameter (Nuclepore, Pleasanton, CA). The filters were pretreated by a brief soaking in 2 mg/ml of poly-L-lysine (molecular weight 3,000) followed by washes with perfusate (14). After filtration, the filters were placed in cold 2% glutaraldehyde, 0.1 M NaPi buffer, pH 7.4, and prepared as described above for scanning electron microscopy, except that a graded ethanol series was employed for dehydration instead of dimethoxypropane.

Chemicals, Enzyme, and Protein Assays: Lactate dehydrogenase activity and protein concentration were determined by standard assays (15, 16). Units of enzyme activity were nmol/min at 23°C. Phalloidin and cytochalasin D were obtained from Boehringer Mannheim Biochemicals (Indianapolis, IN) and Sigma Chemical Co. (St. Louis, MO), respectively. Phalloidin was dissolved directly in perfusate. Cytochalasin D was prepared as a 1 mg/ml stock solution in dimethylsulfoxide and diluted just before use in 50 mg/ml bovine serum albumin (Sigma Chemical Co.; fatty acid free) to a solution of 10 μg/ml which was infused into the perfusion medium with a syringe pump. Other reagents of highest purity were obtained from standard commercial sources.

RESULTS

Adequacy of Perfusion

Livers were perfused at 37°C with Krebs-Henseleit-bicarbonate buffer. A hemoglobin-free perfusate was used so that fluorometric measurements of pyridine nucleotides could be made from the liver surface. The reduced oxygen carrying capacity of this medium was compensated for by bubbling it with oxygen (95% oxygen, 5% carbon dioxide) instead of air and by employing high flow rates (3–4 ml/min/g of liver). Under these conditions, the entire liver lobule was normoxic as determined by several criteria: (*a*) the measured effluent oxygen tension was high (150–250 torr); (*b*) NAD^+ was highly oxidized in both periportal and pericentral regions of the lobule as determined by micro-light guide tissue fluorometry (7) and by direct measurements of NAD^+ and NADH in microdissected periportal and pericentral regions of rapidly frozen livers (F. C. Kauffman and R. G. Thurman, unpublished observations); (*c*) surface oxygen tensions measured directly with miniature oxygen electrodes were high in both periportal and pericentral regions, although periportal oxygen tensions were always higher than pericentral (9); and (*d*) the ultrastructure of periportal and pericentral regions remained normal even after perfusions of an hour or more (10).

The basic organization of the liver parenchyma was apparent in scanning electron micrographs (Figs. 1 and 2). Each hepatocyte possessed three distinct surfaces—canalicular, intercellular, and sinusoidal. Canalicular surfaces of adjacent hepatocytes formed bile canaliculi, narrow channels into which numerous microvilli projected. By comparison, noncanalicular intercellular surfaces were smooth and regular except for peg-like interdigitations between cells and membrane tears corresponding to gap junctional complexes (17). Sinusoidal surfaces faced the overlying sinusoidal endothelium and were densely populated with microvilli that filled the subendothelial space.

Lining the sinusoids was a continuous fenestrated endothelium. Most fenestrations were grouped in clusters and were uniform in size, ~0.15 μm in diameter. Less numerous were larger fenestrations of more variable diameter (1–3 μm) which matched the overall dimensions of the individual clusters of small fenestrations.

Each hepatocyte was adjacent to at least two and often three sinusoids. Typically, the distance from one sinusoidal surface to another was 10–12 μm. Since cellular diameter averaged ~20 μm, no point within a hepatocyte was >10 μm from a sinusoidal surface.

Rapid Bleb Formation during Hypoxia

Perfused livers were made hypoxic by reducing the perfusion flow rate to <1 ml/min/g of liver. Based upon sublobular measurements of NADH fluorescence, stable, circumscribed, centrilobular zones of virtual anoxia developed under these conditions while periportal regions remained normoxic (10). Although NADH fluorescence was not monitored in all the experiments described here, centrilobular injury with periportal sparing developed consistently indicative of the reproducibility of the experimental conditions.

The onset and evolution of centrilobular anoxic injury was followed after 5, 15, 30, and 45 min of hypoxia. After 5 min, centrilobular tissue appeared essentially normal in low power scanning electron micrographs (Fig. 3). At higher power, however, many small processes were observed to project through fenestrations of the endothelium into sinusoids (Fig. 4). These small projections appeared to be microvilli of underlying hepatocytes. The tips of many of these microvilli were swollen. After 15 min of low-flow hypoxia, more obvious structural alterations had developed characterized by large

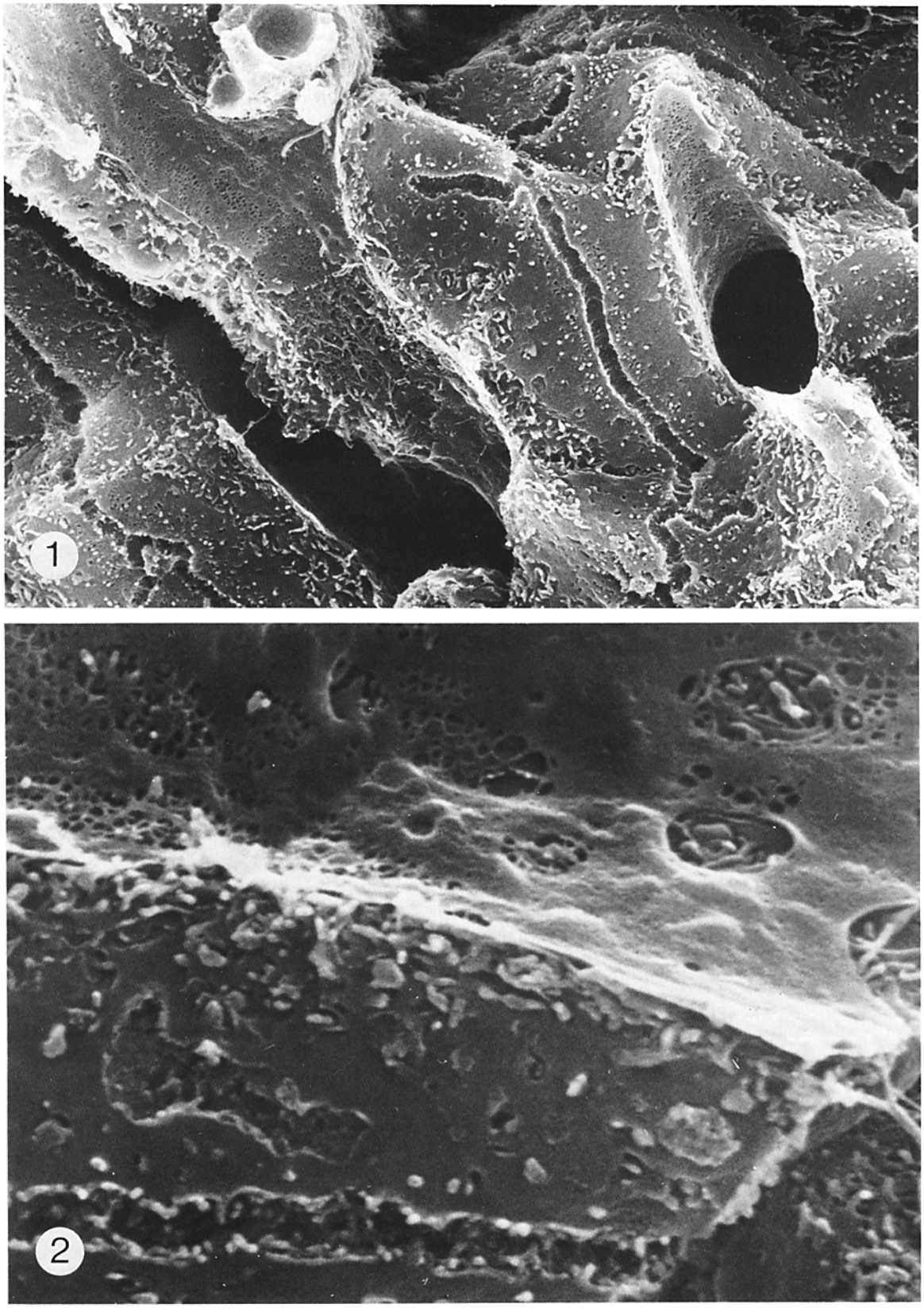

FIGURES 1 and 2 Fig. 1: Scanning electron micrograph of periportal liver tissue after 45 min of low-flow hypoxia (flow rate = 1 ml/min/g of liver) showing normal morphology. Note canalicular, intercellular, and sinusoidal surfaces of the hepatocytes. × 4,000. Fig. 2: Higher power view of normoxic perfused liver. A portion of the lateral surface of a hepatocyte is shown in the lower half of the micrograph. Note the bile canaliculus, many small peg-like processes that interdigitate with adjacent cells, and a membrane tear (lower left) representative of a gap junctional complex. The upper half shows the sinusoidal endothelium. Note large endothelial fenestrations (upper right) and clusters of small fenestrations (upper left). × 14,000.

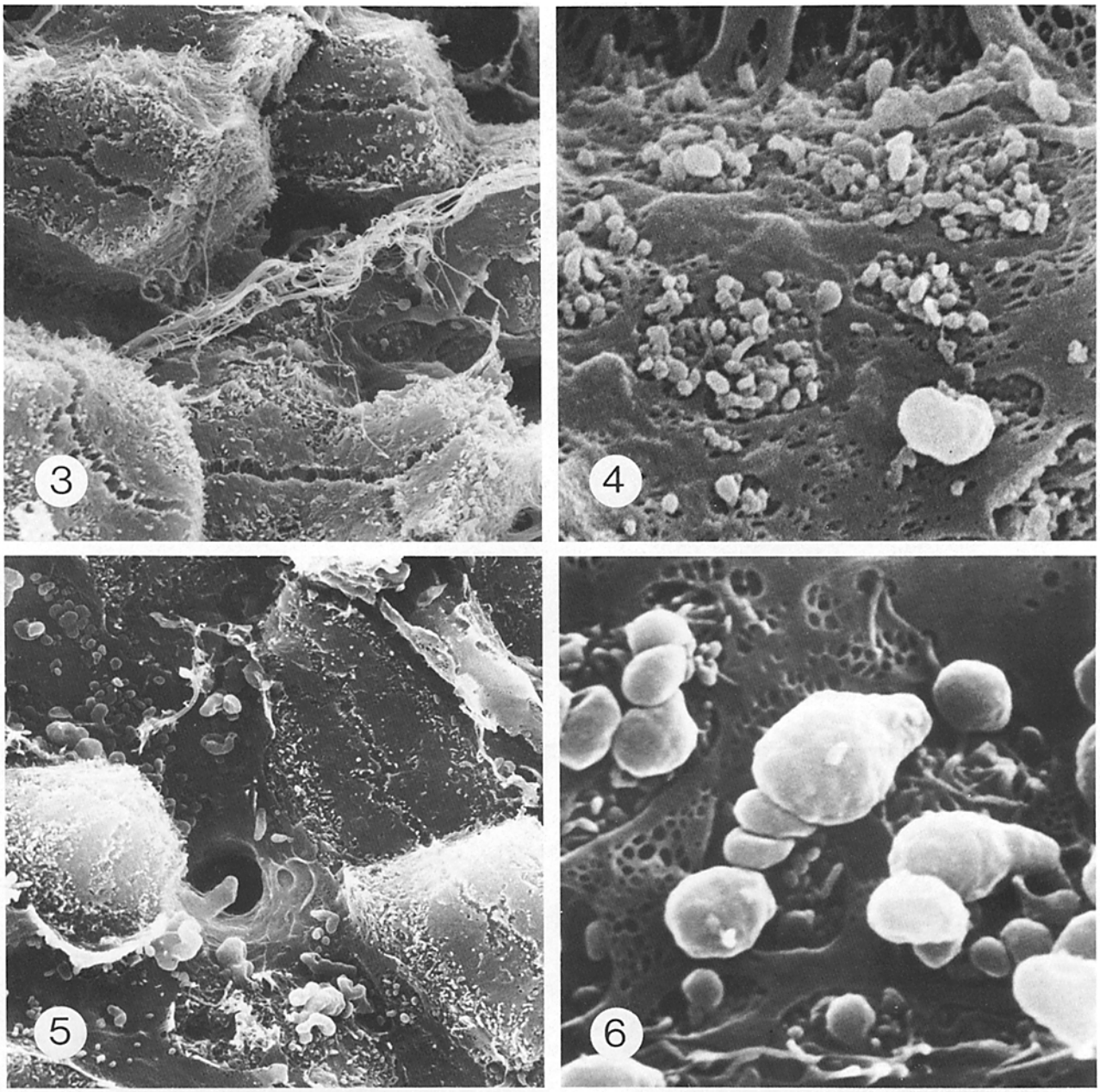

FIGURES 3–6 Fig. 3: Centrilobular region of perfused liver after 5 min of low-flow hypoxia. Little change is evident at this relatively low magnification. × 3,000. Fig. 4: Higher power view of centrilobular region after 5 min of low-flow hypoxia. Note microvilli, some with bulbous tips (lower right), projecting through fenestrations. × 14,000. Fig. 5: Centrilobular region of perfused liver after 15 min of low-flow hypoxia. Blebs projecting into sinusoids are readily identified at low magnification. × 3,000. Fig. 6: Higher power view of centrilobular region after 15 min of low-flow hypoxia. Note blebs projecting into the sinusoidal lumen through fenestrations of the endothelium. Continuity of blebs with underlying hepatocytes can be observed. × 14,000.

bleb-like protrusions into sinusoids (Figs. 5 and 6). Only the sinusoidal surfaces of hepatocytes were affected—the intercellular and canalicular surfaces were essentially unchanged. With increasing duration of hypoxia, there was a steady progression of the injury. By 45 min, virtually all sinusoidal surfaces were covered with blebs (Fig. 7). Other changes included fragmentation of the endothelium and loss of cellular surface detail. Rounding and moderate swelling of hepatocytes was also observed in some micrographs.

We also examined normoxic and anoxic tissue by thin section electron microscopy. In normoxic hepatocytes, microvilli covered the sinusoidal surface, and filamentous structures (microfilaments and microtubules) could be identified in the cortical cytoplasm (Fig. 8). In anoxic regions, blebs covered the sinusoidal surfaces of hepatocytes and projected via slender necks into the sinusoidal space (Fig. 9). Bleb contents were variable. Most contained an amorphous material together with rough or smooth endoplasmic reticulum. Glycogen rosettes and free ribosomes were also found frequently. Larger organelles such as mitochondria, lysosomes, and peroxisomes were never observed in blebs. On sinusoidal surfaces showing blebs, normal microvilli were infrequent and had

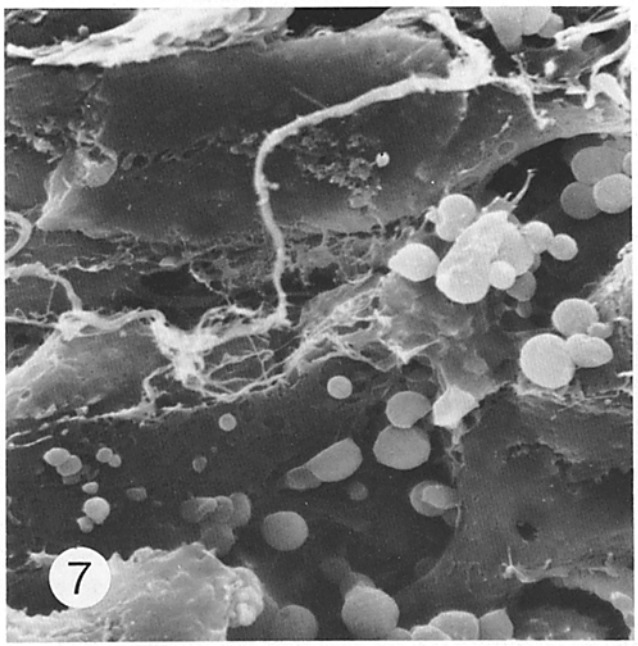

FIGURE 7 Centrilobular region of perfused liver after 45 min of low-flow hypoxia. Blebs remain a prominent feature. In addition, there is loss of most cell surface detail. × 3,000.

apparently been replaced by blebs. The smallest blebs appeared to be microvilli with swollen bulbous tips.

Reversal of Structural Alterations by Reoxygenation (Reflow)

The reversibility of centrilobular structural alterations induced by low-flow hypoxia was investigated by restoring the original flow rate. After 15 min of hypoxia and 15 min of reflow, there was disappearance of blebs, shrinkage of hepatocytes, enlargement of sinusoids, dilation of endothelial fenestrations, and increased tortuosity of the bile canaliculi (Fig. 10). Reflow after 45 min of low-flow hypoxia produced similar results with disappearance of blebs and hepatocellular shrinkage (Fig. 11). In addition, there was considerable recovery of cell surface detail that had been lost after 45 min of hypoxia. The enlargement of sinusoids, dilation of fenestrations, and tortuosity of canaliculi occurring with reflow appeared to be secondary to the marked decrease in hepatocellular volume. Thus, as in heart tissue (18–20), reoxygenation of anoxic liver tissue resulted in an apparent exacerbation of the injury and caused a disruption of cellular volume control.

Release of Protein, Lactate Dehydrogenase, and Cytoplasmic Fragments after Reoxygenation

Since blebs disappeared after reoxygenation, the question arose whether they were resorbed by hepatocytes or released into the circulation. To distinguish between these possibilities, samples of effluent were collected and analyzed for lactate dehydrogenase (LDH) and protein (Fig. 12). LDH released from the perfused liver was low under normal perfusion conditions and remained low or decreased during low-flow hypoxia. After reflow, LDH and protein release increased sharply. After up to 30 min of low-flow hypoxia, reflow produced a transient increase in LDH and protein release followed by a return to baseline levels. After 45 min of low-flow hypoxia, release was sustained after reoxygenation, possibly indicating more severe and irreversible damage.

The appearance of LDH in the effluent perfusate suggested that blebs were released into the microcirculation upon reoxygenation. In an effort to recover blebs, effluents were filtered through polylysine-coated Nuclepore filters of 0.2-μm pore size. The filters were subsequently prepared for scanning electron microscopy. During perfusions at normal flow rates (normoxic perfusion), very little material was recovered from the effluent, and only 0.2-μm pores were visible on the filter surface (Fig. 13). Effluents collected during low flow yielded only slightly more material (Fig. 14). In effluents collected after the resumption of the original rate of flow (reoxygenation) following a low flow period, however, a great deal of material corresponding in size and shape to blebs was recovered (Fig. 15). Larger fragments were also recovered, especially after longer periods of reflow, which seemed to correspond to fragments of desquamated endothelium (Fig. 16).

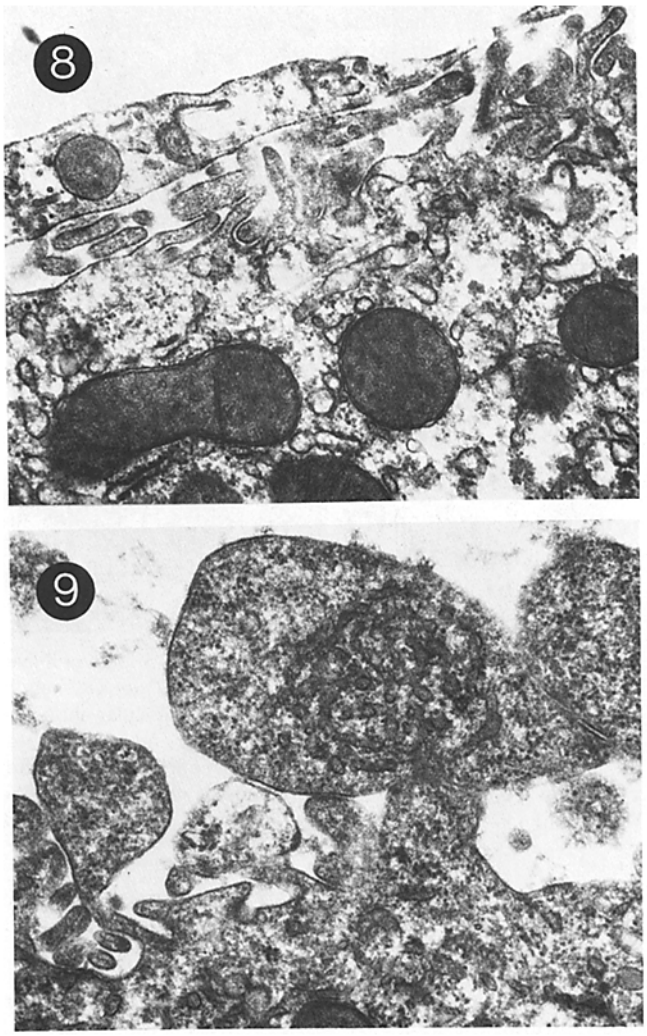

FIGURES 8 and 9 Fig. 8: Transmission electron micrograph of the sinusoidal surface of a normoxic hepatocyte. Note microvilli in the subendothelial space. × 25,000. Fig. 9: Transmission electron micrograph of a centrilobular region of perfused liver after 15 min of low-flow hypoxia. Note bleb-like surface protrusions attached by slender necks to the underlying hepatocyte. × 25,000.

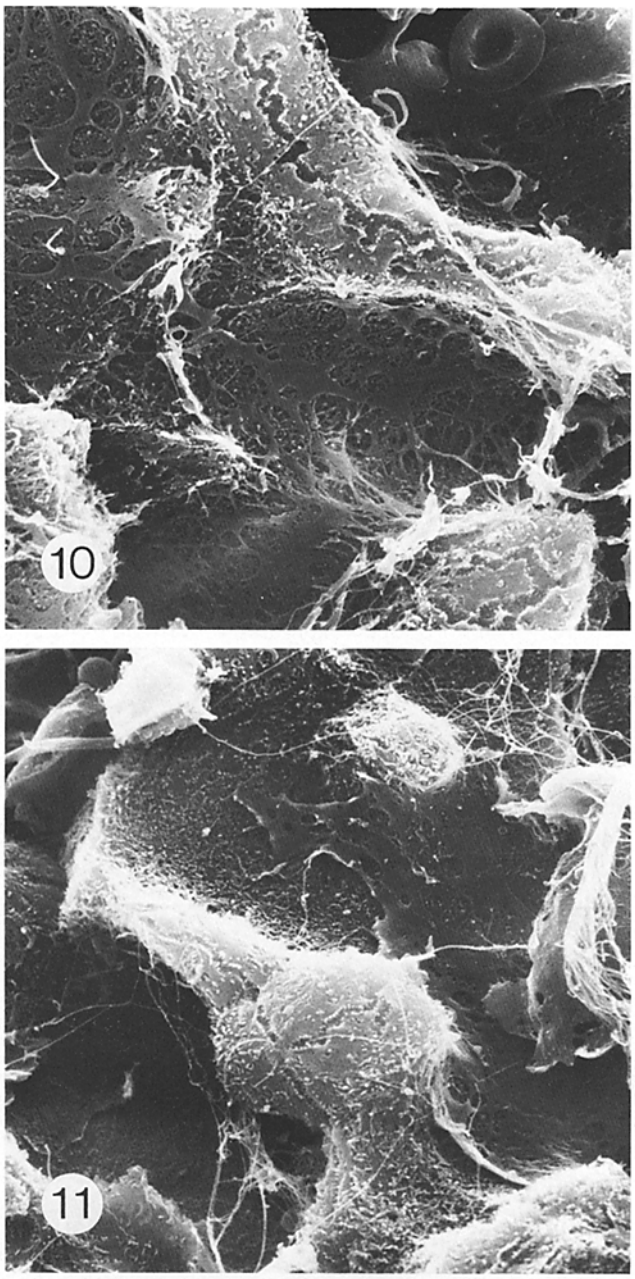

FIGURES 10 and 11 Fig. 10: Centrilobular region of perfused liver after 15 min of low-flow hypoxia and 15 min of reoxygenation. Blebs have disappeared and substantial hepatocellular shrinkage has occurred. Note also the enlargement of the endothelial fenestrations. × 3,000. Fig. 11: Centrilobular region of perfused liver after 45 min of low-flow hypoxia and 15 min of reoxygenation. The endothelium is torn. × 3,000.

In some instances, fenestrations in these larger fragments could be identified (Fig. 16, arrows).

Effects of Phalloidin and Cytochalasin D on Hepatocyte Surface Structure

Since it is widely held that cell surface topography is determined by the organization of cortical microfilaments (21, 22), we examined the effects of phalloidin and cytochalasin D, agents that disrupt the actin cytoskeleton and which produce blebbing in isolated hepatocytes (23, 24). Brief exposures to low concentrations of either toxin produced striking structural alterations. Exposure to phalloidin (1.5 μg/ml in the perfusate for 15 min) produced deep invaginations of hepatocellular surfaces, loss of microvilli and distortion of all cell surface features (Fig. 17). Cytochalasin D treatment (0.25 μg/ml for 15 min) also caused loss of microvilli and disappearance of virtually all surface detail (Fig. 18). However, instead of deep surface invaginations, we observed a marked dilation of the canaliculi. Although both these agents are cytoskeletal disruptors, their effects on liver structure were different, presumably because they interact with the cytoskeleton in different ways.

DISCUSSION

Role of the Cytoskeleton in Hypoxic Hepatocellular Injury

The isolated, hemoglobin-free, perfused rat liver provided a convenient model to study the effects of hypoxia. When oxygen delivery became limiting, stable zones of centrilobular anoxia developed leading to centrilobular injury. Periportal regions remained normoxic and showed normal ultrastructure even after 45 min (Fig. 1). The most prominent feature of hypoxic injury to the perfused liver was an alteration of the cell surface characterized by bleb formation on the sinusoidal surfaces of anoxic centrilobular hepatocytes (Figs. 4–7 and 9). With the formation of blebs, there was loss of microvilli and an apparent disruption of microfilamentous structures of the cortical cytoplasm. Both scanning and transmission electron micrographs indicated that blebs arose by transformation of

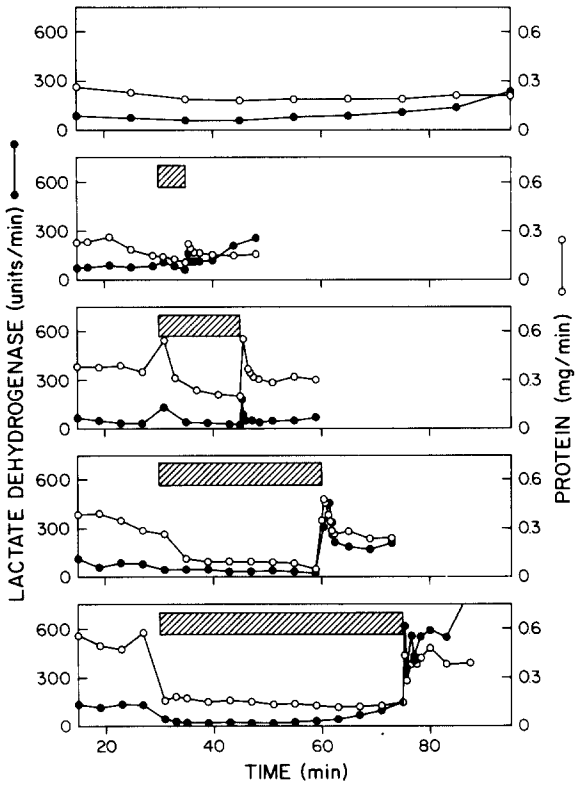

FIGURE 12 Lactate dehydrogenase and protein release into the effluent perfusate after reoxygenation of hypoxic livers. Reflow led to abrupt enzyme and protein release into the effluent, the severity of which was proportional to the duration of low-flow hypoxia. Striped bars indicate periods of low flow.

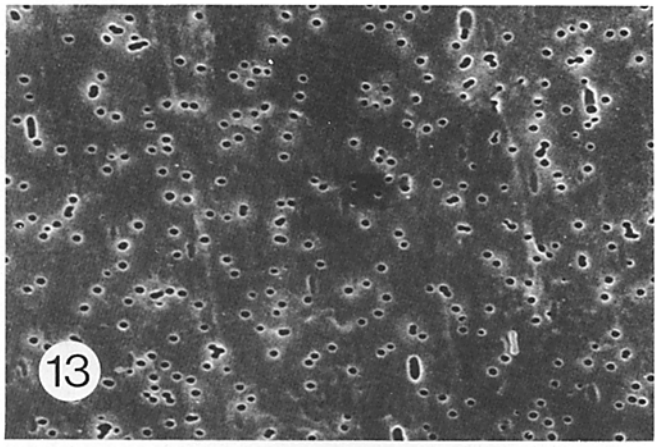

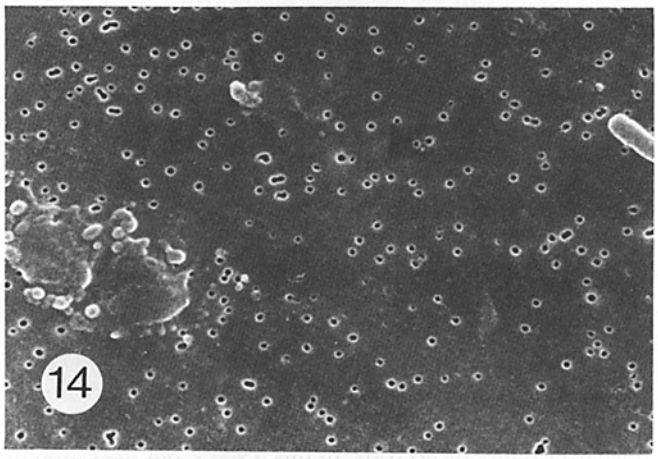

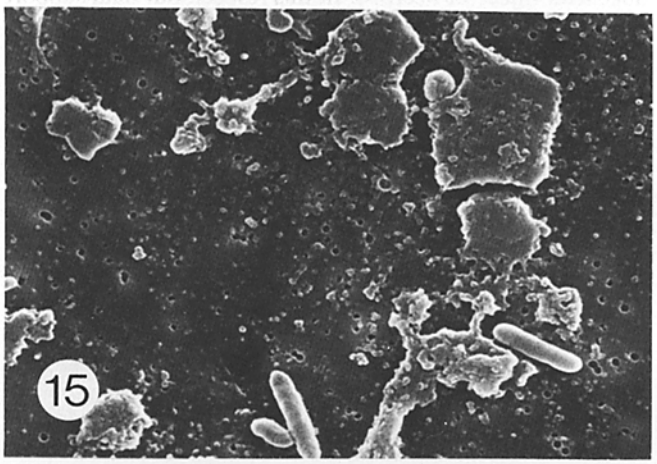

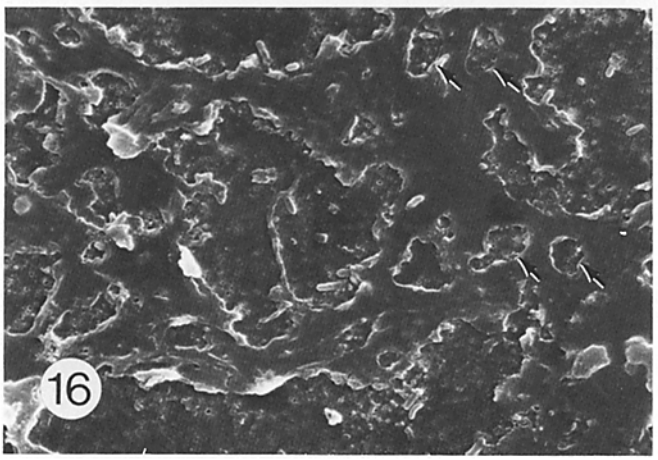

microvilli, since the earliest change seen was swelling of the distal ends of microvilli. This suggests that there was disorganization of the cytoplasmic core of microfilaments within microvilli or a breakdown of membrane-filament attachments.

The importance of the cytoskeleton as a determinant of cell surface topography was underscored by the rapid and profound alterations of cell surface structure caused by the cytoskeletal disrupters, phalloidin and cytochalasin D (21 and 22). Phalloidin, which stabilizes microfilaments, caused extensive invagination of the cell surface and vacuolization of the cytoplasm (Fig. 17). Cytochalasin D, which causes depolymerization of actin microfilaments, produced disappearance of the microvilli, loss of nearly all cell surface detail, but little surface invagination (Fig. 18). Neither drug caused bleb formation in the perfused liver, although both drugs induce blebbing in isolated hepatocytes (23 and 24). Many of the changes we observed by scanning electron microscopy in the isolated liver resembled those reported by others using transmission electron microscopy (25 and 26). Scanning electron microscopy, however, revealed differences in the effects of the two drugs which were not observed with transmission electron microscopy alone (26). The rapidity and severity of the structural alterations produced by these agents indicate that the hepatic cytoskeleton is not an inert, rigid structure but that it is labile and in a state of continuous turnover. Hypoxic injury in the perfused liver, although resembling the effects of cytochalasin D and phalloidin on isolated hepatocytes, did not mimic the effect of either drug on the intact organ.

Reversibility and Paradoxical Exacerbation of Hypoxic Injury

Hypoxic injury was aggravated by reoxygenation, not simply reversed. In particular, reoxygenation produced release of blebs as cytoplasmic fragments (Figs. 15 and 16) and caused marked shrinkage of hepatocytes (Figs. 10 and 11). The latter effect appears to be comparable to the reperfusion paradox observed in cardiac tissue in which reperfusion of ischemic tissue exacerbates injury and causes a disruption of volume regulation (18–20). Calcium seems to play an important role in the reperfusion paradox by entering cells after reperfusion and interfering with a number of cellular functions including mitochondrial oxidative phosphorylation (27, 28). Calcium

FIGURES 13–16 Fig. 13: Scanning electron micrograph of a polylysine-coated Nuclepore filter after passage of effluent from normoxic liver. Effluent was collected for 10 min from a normoxic perfused liver immediately prior to the beginning of low-flow hypoxia. The filter surface is clear. × 6,000. Fig. 14: Nuclepore filter after passage of effluent from liver following low-flow hypoxia. Effluent was collected during the last 10 min of 30 min of low-flow hypoxia in the same experiment as Fig. 14. Only a small amount of material was recovered on the filter surface. × 6,000. Fig. 15: Nuclepore filter after passage of effluent from reoxygenated liver. Effluent was collected during the first 10 min of reoxygenation after 30 min of low-flow hypoxia in the same experiment as Fig. 14. Considerable polymorphous material was recovered on the filter surface. × 6,000. Fig. 16: Nuclepore filter after passage of effluent obtained after prolonged reoxygenation of hypoxic liver. Effluent was collected between 20 and 30 min after reoxygenation in the same experiment as Fig. 14. Note large, flat structures with fenestrations (arrowheads) which appear to be desquamated endothelial cells. × 1,900.

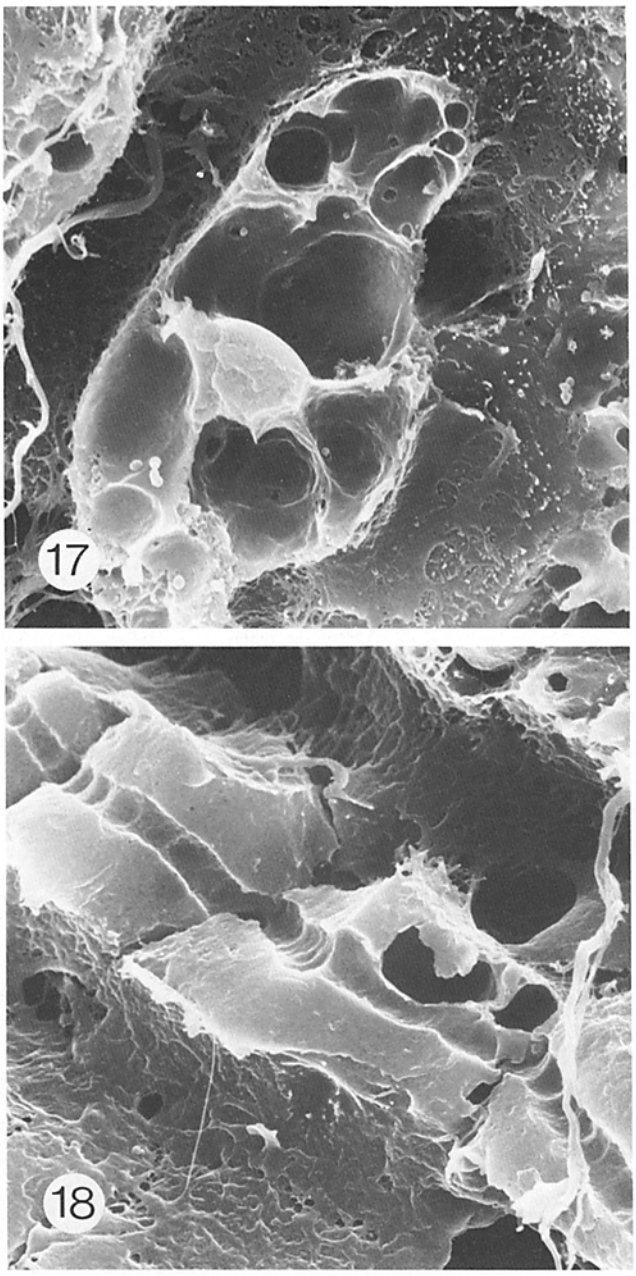

FIGURES 17 and 18 Fig. 17: Perfused liver after 15 min of exposure to phalloidin (1.5 μg/ml in the perfusate). Note deep invaginations of hepatocellular surfaces. × 3,000. Fig. 18: Perfused liver after 15 min of exposure to cytochalasin D (0.25 μg/ml in the perfusate). Note complete loss of microvilli. × 3,000.

may also play an important role in bleb formation, since cytosolic calcium is an important regulator of cytoskeletal structure and function (29). Studies on the role of calcium in hepatic injury caused by hypoxia and reoxygenation are currently underway.

Changes in hepatocellular volume were accompanied by reciprocal changes in the size of sinusoids (Figs. 10 and 11). Thus, the surface area of the sinusoidal walls increased as hepatocytes shrank. This increase of lumenal surface area was accounted for by an increase in the size of endothelial fenestrations. Two processes seemed to occur. First, clusters of 20 to 40 small fenestrations, each ~0.15 μm in diameter, coalesced to form single large fenestrations of 1–3 μm in diameter. Second, there was further expansion of large fenestrations. After the most severe hepatocellular shrinkage, the endothelium consisted almost entirely of thin cords of cytoplasm outlining large, oval gaps. There was a limit to the extent to which the endothelium could accommodate these changes in surface area. After prolonged centrilobular anoxia followed by reoxygenation, especially, considerable tearing of the endothelium occurred and fragments of endothelium were recovered from effluent perfusates (Fig. 16). Another factor influencing the size of fenestrations may be perfusion pressure. In a few experiments in which outflow was inadvertently obstructed, clusters of small fenestrations appeared to coalesce into single large fenestrations in response to the increase of intraluminal pressure and resultant increase in vessel diameter.

The structure of the perfused liver was quite stable as long as normoxic conditions were maintained, and our morphologic findings by scanning electron microscopy agreed well with earlier reports (17, 30, 31). However, certain features of liver structure were particularly unstable. Thus, micrographs showing sinusoidal blebs or a predominance of large fenestrations should be interpreted with some caution, since these features might easily come about as a consequence of hypoxia or of excessive perfusion pressure during fixation.

Vulnerability of Hepatocytes to Hypoxic Injury

Our studies support fully the expectation that hypoxia will lead preferentially to injury of centrilobular regions of the liver lobule. Further, we expect that relatively brief periods of centrilobular anoxia (15–45 min) would be sufficient to induce liver injury or necrosis. In this respect, our data support Israel et al.'s contention (6) that ethanol-induced hepatic injury comes about by an ethanol-induced increase in hepatic oxygen uptake. Since we used livers from fed animals which have a high capacity for glycolysis, the postulated glycolytic adaptation of centrilobular hepatocytes (4) appears to provide little protection against hypoxic injury. The importance of oxygen delivery is further underscored by the intimate association of hepatocytes with blood vessels. Each hepatocyte was adjacent to at least two sinusoids, and no point within the hepatocyte was more than ~10 μm from a sinusoidal surface. Thus, the design of the microvasculature serves to minimize the distance of oxygen diffusion from sinusoid to cell.

Hepatic Enzyme Release by Cytoplasmic Shedding

There are several reports of surface bleb formation (also called zeiosis or apoptosis) following various types of toxic and metabolic injury to tissues and isolated cells (cf. references 10, 32–35). The present study is the first to show that bleb formation reverses rapidly with the release of blebs as cytoplasmic fragments. It is well established that enzyme release from injured liver tissue occurs even in the absence of outright hepatic necrosis (36), although the mechanism of this phenomenon is not understood. Our observations suggest that hepatic enzymes can be released from viable tissue through shedding of cell surface blebs. Since blebs contain mostly cytosol and exclude larger organelles such as mitochondria, a shedding mechanism explains how cytosolic enzymes such as glutamate-pyruvate transaminase and lactate dehydrogenase can be released selectively after mild or moderate cellular

injury. In severe liver injury leading to necrosis, both mitochondrial and cytosolic enzymes appear in the blood. Presumably, this occurs through a generalized breakdown of the plasma membrane permeability barrier leading to indiscriminate release of cellular contents.

This work was supported by National Institutes of Health grants AM-30874, GM-28999, and AA-03624 and by a grant-in-aid from the American Heart Association with funds contributed in part by the North Carolina Heart Association. J. J. Lemasters is an Established Investigator of the American Heart Association and R. G. Thurman is the recipient of Career Development Award AA-00033.

Received for publication 17 December 1982, and in revised form 11 April 1983.

REFERENCES

1. Lautt, W. W. 1976. Method for measuring hepatic uptake of oxygen or other bloodborne substance *in situ*. *J. Appl. Physiol.* 40:269–274.
2. Rappaport, A. M. 1976. The microcirculatory acinar concept of normal and pathological hepatic structure. *Beitr. Pathol.* 157:215–243.
3. Loud, A. V. 1968. A quantitative stereological description of the ultrastructure of normal rat liver parenchymal cells. *J. Cell Biol.* 37:27–46.
4. Jungermann, K., and D. Sasse. 1978. Heterogeneity of liver parenchymal cells. *Trends Biochem. Sci.* 3:198–202.
5. MacSween, R. N. M., P. P. Anthony, and P. J. Scheuer, editors. 1979. Pathology of the Liver. Churchill Livingstone, Edinburgh.
6. Israel, Y., H. Kalant, H. Orrego, J. M. Khanna, L. Videla, and J. M. Phillips. 1975. Experimental alcohol-induced hepatic necrosis: suppression by propylthiouracil. *Proc. Natl. Acad. Sci. USA* 72:1137–1141.
7. Ji, S., J. J. Lemasters, and R. G. Thurman. 1980. A non-invasive method to study metabolic events within sublobular regions of hemoglobin-free perfused liver. *FEBS (Fed. Eur. Biochem. Soc.) Lett.* 113:37–41.
8. Ji, S., J. J. Lemasters, and R. G. Thurman. 1981. A fluorometric method to measure sublobular rates of mixed-function oxidation in the hemoglobin-free perfused rat liver. *Molc. Pharmacol.* 19:513–516.
9. Ji, S., J. J. Lemasters, V. Christenson, and R. G. Thurman. 1982. Periportal and pericentral pyridine nucleotide fluorescence from the surface of the perfused liver: evaluation of the hypothesis that chronic treatment with ethanol produces pericentral hypoxia. *Proc. Natl. Acad. Sci. USA.* 79:5415–5419.
10. Lemasters, J. J., S. Ji, and R. G. Thurman. 1981. Centrilobular injury following hypoxia in isolated, perfused rat liver. *Science (Wash. DC).* 213:661–663.
11. Scholz, R., W. Hansen, and R. G. Thurman. 1973. Interaction of mixed-function oxidation with biosynthetic processes. I. Inhibition of gluconeogenesis by aminopyrine in perfused rat liver. *Eur. J. Biochem.* 38:64–72.
12. Estabrook, R. W. 1967. Mitochondrial respiratory control and the polarographic measurement of ADP:O ratios. *Methods Enzymol.* 10:41–47.
13. Chance, B., J. R. Williamson, D. Jamieson, and B. Schoener. 1965. Properties and kinetics of reduced pyridine nucleotide fluorescence of the isolated and in vivo rat heart. *Biochem. Z.* 341:357–377.
14. Williams, R. C. 1977. Use of polylysine for adsorption of nucleic acids and enzymes to electron microscope specimen films. *Proc. Natl. Acad. Sci. USA.* 74:2311–2315.
15. Bergmeyer, H. U. 1974. Methods of Enzymatic Analysis. Academic Press, Inc., New York.
16. Lowry, O. H., N. J. Rosebrough, A. L. Farr, and R. J. Randall. 1951. Protein measurement with the folin phenol reagent. *J. Biol. Chem.* 193:265–275.
17. Meyer, D. J., S. B. Yancey, J.-P. Revel, and A. Peskoff. 1981. Intercellular communication in normal and regenerating rat liver: a quantitative analysis. *J. Cell Biol.* 91:505–523.
18. Whalen, D. A., D. G. Hamilton, C. E. Ganote, and R. B. Jennings. 1974. Effect of a transient period of ischemia on myocardial cells. I. Effects on cell volume regulation. *Am. J. Pathol.* 74:381–398.
19. Kloner, R. A., C. E. Ganote, D. A. Whalen, and R. B. Jennings. 1974. Effect of a transient period of ischemia on myocardial cells. II. Fine structure during the first few minutes of reflow. *Am. J. Pathol.* 74:399–422.
20. Hearse, D. J., S. M. Humphrey, W. G. Nayler, A. Slade, and D. Border. 1975. Ultrastructural damage associated with reoxygenation of the anoxic myocardium. *J. Mol. Cell. Cardiol.* 7:315–324.
21. Weihing, R. R. 1979. The cytoskeleton and plasma membrane. *Methods Achiev. Exp. Pathol.* 8:42–109.
22. Weatherbee, J. A. 1981. Membranes and cell movement: Interaction of membranes with the proteins of the cytoskeleton. *Int. Rev. Cytol.* 12(Suppl.):113–176.
23. Weiss, E., I. Sterz, M. Frimmer, and R. Kroker. 1973. Electron microscopy of isolated rat hepatocytes before and after treatment with phalloidin. *Beitr. Pathol.* 150:345–356.
24. Prentki, M., C. Chaponnier, B. Jeanrenaud, and G. Gabbiani. 1979. Actin microfilaments, cell shape, and secretory processes in isolated rat hepatocytes. Effect of phalloidin and cytochalasin D. *J. Cell Biol.* 81:592–607.
25. Miller, F., and O. Wieland. 1967. Electron microscopic studies of mouse and rat hepatic cells after acute phalloidin poisoning. *Virchows Arch. Pathol. Anat.* 343:83–99.
26. Jahn, W. 1979. Cytochalasin D is able to mimic the effects of phalloidin in the rat liver. *Experientia (Basel).* 35:1638–1639.
27. Hearse, D. J., S. M. Humphrey, and G. R. Bullock. 1978. The oxygen paradox and the calcium paradox: Two facets of the same problem? *J. Mol. Cell Cardiol.* 10:641–668.
28. Mittnacht, S., S. C. Sherman, and J. L. Farber. 1979. Reversal of ischemic mitochondrial dysfunction. *J. Biol. Chem.* 254:9871–9878.
29. Burridge, K., and J. R. Feramisco. 1981. Non-muscle alpha-actinins are calcium-sensitive actin-binding proteins. *Nature (Lond.).* 294:565–567.
30. Motta, P., and K. R. Porter. 1974. Structure of rat liver sinusoids and associated tissue spaces as revealed by scanning electron microscopy. *Cell Tissue Res.* 148:111–125.
31. Grisham, J. W., W. Nopanitaya, J. Compagno, and A. E. H. Nagel. 1975. Scanning electron microscopy of normal rat liver: the surface structure of its cells and tissue components. *Am. J. Anat.* 144:295–321.
32. Wyllie, A. H., J. F. R. Kerr, and A. R. Currie. 1980. Cell death: the significance of apoptosis. *Int. Rev. Cytol.* 68:251–306.
33. Trump, B. F., A. Penttila, and I. K. Berezesky. 1979. Studies on cell surface conformation following injury. I. Scanning and transmission electron microscopy of cell surface changes following *p*-chloromercuribenzene sulfonic acid (PCMBS)-induced injury of Ehrlich ascites tumor cells. *Virchows Arch. B. Cell Pathol.* 29:281–296.
34. Trump, B. F., A. Penttila, and I. K. Berezesky. 1979. Studies on cell surface conformation following injury. II. Scanning and transmission electron microscopy of cell surface changes following anoxic injury in Ehrlich ascites tumor cells. *Virch. Arch. B. Cell Pathol.* 29:297–307.
35. Sanderson, C. J. 1976. The mechanism of T cell mediated cytotoxicity. II. Morphological studies of cell death by time-lapse microcinematography. *Proc. R. Soc. Lond. B Biol. Sci.* 192:241–255.
36. Zilva, J. F., and P. R. Pannall. 1975. Clinical Chemistry in Diagnosis and Treatment. Year Book Medical Publishers, Chicago.